TecnoLógicas

ISSN-p: 0123-7799
ISSN-e: 2256-5337

Vol. 26, nro. 58, e2765, 2023

Recibido: 22 junio 2023
Aceptado: 23 diciembre 2023
Disponible: 29 diciembre 2023

Evaluation of Bactericidal Activity of Electrochemical GO Modified with TiO_2 Nanoparticles

Evaluación de la actividad bactericida de GO electroquímico modificado con nanopartículas de TiO_2

Geraldine Durango Giraldo[1];
Juan Camilo Zapata-Hernández[2];
Claudia Betancur Henao[3];
Juan F. Santa Marín[4];
Robinson Buitrago Sierra[5]

[1] Instituto Tecnológico Metropolitano, Medellín – Colombia, Universidad Politécnica de Catalunya, Barcelona – España
geraldinedurango189834@correo.itm.edu.co
[2] Instituto Tecnológico Metropolitano, Medellín – Colombia,
juanzapatah@itm.edu.co
[3] Instituto Tecnológico Metropolitano, Medellín – Colombia,
claudiabetancur@itm.edu.co
[4] Instituto Tecnológico Metropolitano, Medellín – Colombia, Universidad Nacional de Colombia, Medellín – Colombia
juansanta@itm.edu.co
[5] Instituto Tecnológico Metropolitano, Medellín – Colombia,
robinsonbuitrago@itm.edu.co

How to cite / Cómo citar

G. Durango Giraldo, J.C. Zapata-Hernández, C. Betancur Henao, J.F. Santa Marín, R. Buitrago Sierra "Evaluation of Bactericidal Activity of Electrochemical GO Modified with TiO_2 Nanoparticles," *TecnoLógicas*, vol. 26, nro. 58, e2765, 2023.
https://doi.org/10.22430/22565337.2765

Abstract

Recently, antibacterial materials have sparked a renewed interest in the fields of biomedical engineering and life sciences. The main purpose of this study was to evaluate the physicochemical properties of TiO_2 nanoparticles with anatase phase and an average size of 24.1 ± 4.6 nm, graphene oxide (GO) obtained from the electrochemical method, and TiO_2/GO hybrid nanomaterial. Thermogravimetric analysis (TGA) revealed the presence of oxygen functionalities in the GO structure and 23.2 % of TiO_2 in the hybrid nanomaterial, as well as a strong interaction between the materials that can be observed in the micrograph of scanning electron microscopy (SEM). Antibacterial tests were performed using the macrodilution method. The results showed that, while GO did not decrease bacterial growth, TiO_2 presented high bactericidal activity. In turn, the hybrid TiO_2/GO nanomaterial did not show such activity. This result can be explained by the decrease in contact between TiO_2 and bacterial cells due to the blocking of the active sites on the TiO_2 surface by graphene oxide sheets. These results contribute to the ongoing discussion about the bactericidal properties of graphene oxide.

Keywords

Bactericidal activity, hybrid nanomaterial, graphene oxide, titanium dioxide.

Resumen

Recientemente, los materiales antibacterianos han despertado un renovado interés en el campo de la ingeniería biomédica y las ciencias de la vida. El objetivo de este estudio consistió en evaluar las propiedades fisicoquímicas de nanopartículas de TiO_2 fase anatasa y un tamaño medio de 24.1 ± 4.6 nm, óxido de grafeno (GO) obtenido a partir del método electroquímico y un nanomaterial híbrido TiO_2/GO. El análisis termogravimétrico (TGA) reveló la presencia de funcionalidades de oxígeno en la estructura del GO, y se encontró un 23.2 % de TiO_2 en el nanomaterial híbrido y una fuerte interacción entre los materiales que puede observarse en las micrografías de microscopia electrónica de barrido (SEM). Las pruebas antibacterianas fueron realizadas usando el método de macrodilución. Los resultados evidenciaron que, mientras que el GO no disminuyó el crecimiento bacteriano, el TiO_2 presentó una alta actividad bactericida. A su vez, el nanomaterial híbrido TiO_2/GO no mostró dicha actividad. Este resultado puede explicarse por la disminución del contacto entre el TiO_2 y las células bacterianas debido al bloqueo de los sitios activos en la superficie del TiO_2 por las láminas de óxido de grafeno. Estos resultados contribuyen a la discusión en curso sobre las propiedades bactericidas del óxido de grafeno.

Palabras clave

Actividad bactericida, nanomaterial híbrido, óxido de grafeno, dióxido de titanio.

1. INTRODUCTION

Health-care-associated infections, which are acquired during hospital stays, could represent a serious risk to human health [1]. The pathogens responsible for this kind of infections (also known as nosocomial) include bacteria, viruses, and fungi. The most common bacterium is *Escherichia coli (E.Coli),* and it causes acute urinary tract infections, urinary tract sepsis, and neonatal meningitis [2]. The World Health Organization (WHO) estimates that, in North America and Europe, nosocomial infections cause 5 % and 10 % of the hospitalizations, respectively. In Latin America and Asia, the proportion of hospitalizations due to the same cause is approximately 40 % [3].

Accordingly, the general interest in developing antibacterial materials has grown in recent years. Hybrid nanomaterials have potential in this regard because they facilitate the use of nanostructured materials with specific properties and excellent mechanical properties, as well as improved biocompatibility and antibacterial activity. This makes them good prospects in tissue engineering [4].

On the one hand, graphene oxide (GO) has attracted special attention because it is a carbon atom monolayer that forms a dense honeycomb structure containing carboxylic groups on the edges, as well as hydroxyl and epoxide groups on its two accessible sides. GO has excellent physicochemical properties, large specific surface, mechanical resistance, electrical conductivity, and stability in water [5], [6]. However, its antibacterial activity is quite controversial, and some authors have shown that it is related to the size and shape of GO [7], [8].

Nowadays, Hummers' method is the most widely implemented strategy to synthesize GO used in bacterial applications [9], [10]. Nevertheless, it uses dangerous reagents that are harmful to the environment and humans [11]. Electrochemical exfoliation of graphite is an alternative method for obtaining graphene oxide; it is simple and requires less reagents for the synthesis process than Hummers' method [12], [13].

On the other hand, titanium dioxide (TiO_2) is considered a suitable material for medical applications due to its low toxicity, excellent thermal properties, and chemical stability. Additionally, TiO_2 exhibits antibacterial activity against *E. Coli* due to oxidative damage to the cell membrane [14], [15]. Thanks to these properties, TiO_2 has been used in several applications, such as microbatteries and as UV absorber in cosmetic products, anticorrosive coating, and antibacterial coatings [16], [17].

The main objective of this study was to evaluate the antibacterial activity of synthesized graphene oxide (GO), titanium dioxide (TiO_2) and a TiO_2/GO hybrid. The combination of two types of nanoparticles with different morphologies and dimensions is a new way to produce functional hybrid materials with a synergistic improvement in material performance.

Recently, several hybrids composed of GO and conventional semiconductors demonstrated significantly enhanced photocatalytic performance during pollutant degradation. Specifically, TiO_2/GO is a hybrid that could be considered as a promising material photocatalysis and hydrogen evolution [18]–[20], solar mineralization [21], and others fields of engineering such as tissue engineering as hybrid filler of functional nanocomposites [22].

Escherichia coli was the model bacteria used here to evaluate the bactericidal effect of the three materials. This study was conducted to contribute to the ongoing discussion about the antibacterial properties of GO. In addition, to the best of the authors' knowledge, the antibacterial properties of GO synthetized by the electrochemical method had not been reported before. The electrochemical method can be used as an alternative to produce GO because it is sustainable and more environmentally friendly.

2. METHODOLOGICAL ASPECTS

2.1 Materials

All the materials employed here were reagent-grade and used without any further purification. Titanium isopropoxide ($Ti[OCH(CH_3)_2]_4$, 97 %, Sigma-Aldrich), ethanol (99.5 % J.T Baker), high-purity graphite rods (3x305 mm, 99.9 %, SPI supplies), sulfuric acid (H_2SO_4, 96 %, Fisher Scientific) and sodium sulfate (Na_2SO_4, 99 %, Chemi) were used for the synthesis of TiO_2 and graphene oxide. All the solutions were prepared using deionized water.

2.2 Methods

2.2.1 TiO_2 synthesis

TiO_2 nanoparticles were synthesized by the hydrothermal method [23]. A total of 10 mL of titanium isopropoxide (TTIP) were added to 13.3 mL of ethanol under constant stirring; then, 16.6 mL of deionized water were added slowly drop by drop to the TTIP-ethanol solution under constant stirring. The white precipitate thus obtained was stirred for 2 h, transferred to a Teflon autoclave, and heated at 80 °C for 4 h in an oven furnace (Binder, KB 105). After that, the autoclave was allowed to cool down to room temperature, and the material was filtered and dried overnight at 80 °C. Finally, said material was calcinated at 400 °C for 4 h in a tube furnace (Nabertherm, P 330) to favor the formation of the crystalline phase anatase and remove waste products.

2.2.2 GO synthesis:

GO was synthesized by the electrochemical exfoliation method. An electrolyte solution of Na_2SO_4 at 0.1 M was prepared in deionized water and the pH was adjusted (~6.5 to 7) with H_2SO_4. Then, two graphite rods were immersed in the electrolyte solution using a working distance of 20 mm, and they were connected to a DC voltage source (10 V). Finally, the product was washed several times with water and ethanol and dried in an oven at 80 °C.

2.2.3 TiO_2/GO composite synthesis

The TiO_2/GO composite was prepared mixing the materials previously synthesized in a 1:3 wt. % ratio using a Q500 Sonicator (20 kHz, Qsonica LLC, USA). The ultra-sonication probe tip was immersed directly in the suspension, and the supplied energy was adjusted at 30 % of the maximum capacity in order to avoid heating problems. Ultrasound pulses were applied 1 s ON and 2 s OFF during 15 minutes. Finally, the sample was filtered and dried in an oven at 80 °C.

2.2.4 Antimicrobial test

The antimicrobial activity of TiO_2,GO and the TiO_2/GO hybrid nanomaterial was evaluated using the macrodilution method, as described in our previous paper [24]. *Escherichia coli* (ATCC 25922) was selected as gram-negative bacteria model. For each experiment, bacterial stocks were grown in BHI (Brain Heart Infusion) for 24 hours in an incubator at 37 °C and 80 % relative humidity. Later, the inoculum was prepared in the range reported in McFarland's standard No. 0.5 (1–2 x 10^8 CFU/ml; OD at 625 nm: 0.08–0.13) [25].

For the test of bactericidal activity, dilutions of different concentrations (1000, 500, 250 and 125 μg/mL) of TiO_2, GO and TiO_2/GO were prepared. After that, 10 μL of the inoculum were placed into 2 mL tubes containing 1.5 mL of each dilution prepared. As control sample, 10 μL of bacteria inoculum were placed in BHI. After that, the materials were incubated at 37 °C and 80 % relative humidity for 24 h under constant agitation. Bacterial concentrations were determined by measuring optical densities (ODs) at 625 nm with a spectrophotometer (8453A, Agilent). All the experiments were performed in triplicate. Bacterial viability was calculated using (1).

$$Bacterial\ viability\ (\%) = \frac{sample\ OD}{control\ OD} x100 \quad (1)$$

Where sample OD is the absorbance of each sample tested with the material dilutions, and control OD is the optical absorbance of the untreated sample.

The Minimum Inhibitory Concentration (MIC) required to inhibit the growth of 50 % of organisms (MIC50) was calculated using and the selection criterion was $R^2 \geq 0.99$.

2.3 Physical-chemical characterization

The phase identification and lattice structure characterization of the synthesized TiO_2 were performed using an X-ray diffractometer (PANalytical Empyrean Series II), operated with Cu Kα radiation (λ = 1,540 Å). The thermal stability was characterized by thermogravimetric analysis (TGA) using a discovery 550 Thermogravimetric Analyzer with a heating program, initially, under a nitrogen atmosphere up to 800 °C. Subsequently, the atmosphere was changed to air. The functional groups present in the samples were analyzed by infrared spectroscopy in a IRTracer-100 spectrophotometer with wavelengths between 500 and 4000 cm^{-1}. The numbers of defects and layers in the GO were estimated by a LabRAM HR Raman spectrometer (Horiba-Jobin Yvon). [26] The structural morphology of the particles was evaluated using a JEOL 7100F scanning electron microscope (FE-SEM) and transmission electron microscopy (TEM) in a TMP-FEI equipment.

3. RESULTS AND DISCUSSION

Figure 1a and 1b show the X-ray diffraction pattern of TiO_2 nanoparticles and the Raman spectra of graphene oxide, respectively. The XRD pattern (Figure. 1a) shows anatase-phase TiO_2 with characteristic diffraction peaks of 20 values at about 25.3°, 37.8°, 48°, 53.9° and 55°, they are attributed to the (101), (004), (200), (105) and (211) planes, respectively. These results are in agreement with those reported by. [27] and match standard ICDD card No. 01-073-1764 for anatase.

Figure 1b shows the Raman spectra of graphene oxide, with three characteristic bands: D-band (~1339 cm^{-1}), G- band (~1583 cm^{-1}) and 2D-band (~2686 cm^{-1}). The G-band represents the sp^2 hybridization of carbon atoms [28], while the D-band is related to changes in the hybridization of carbon atoms (sp^2 to sp^3) [29]. The change in the hybridization can be related to oxygen functionalities in graphene oxide [30]. The D/G ratio is commonly used to evaluate the number of defects in graphene oxide. The GO obtained here exhibited a D/G ratio of 0.61, which is consistent with what was found [31]. Additionally, this D/G ratio is lower than that of the GO obtained by Hummers' method [32], [33]. The 2D/G ratio is used to estimate the

number of layers in graphene oxide. In this case, the GO presented a 2D/G ratio of 1.41, which suggests the presence of bilayer graphene oxide [34].

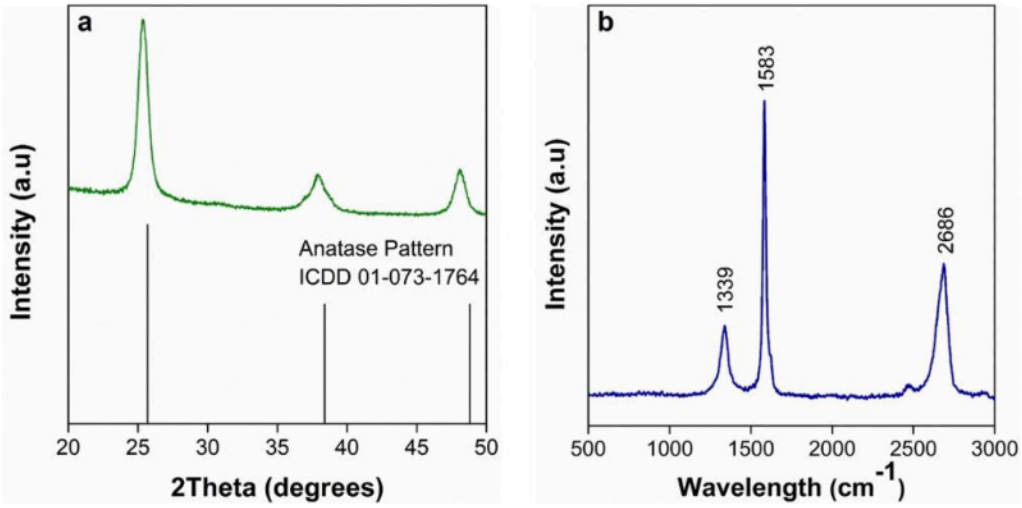

Figure 1. (a) XRD pattern of TiO_2 nanoparticles; (b) Raman spectra of GO. Source: Own elaboration.

Figure 2 shows the FTIR spectra of TiO_2, GO and the TiO_2/GO composite obtained in this study. All the samples present a band between 3000 cm^{-1} and 3377 cm^{-1}, which corresponds to the stretching vibration of the O-H bond. The spectrum of TiO_2 shows a band around 1610 cm^{-1} related to the bending vibration mode of the O-H bond, and characteristic bands of titanium dioxide are located at 400 cm^{-1} and 800 cm^{-1}. The spectrum of GO shows several bands, but the one at 2939 cm^{-1} is due to C-H stretching vibration, which occurs during the synthesis process [35]. The bands at 1380 cm^{-1}, 1220 cm^{-1} and 1060 cm^{-1} correspond to C-O, C-OH and C=O functional groups [36], [37]. The spectrum of TiO_2/GO exhibits new bands at 1690 cm^{-1} and 1155 cm^{-1}, which are related to C=O and Ti-O-C cm^{-1}, respectively [38]. The presence of Ti-O-C and C=O functional groups demonstrated the interaction between oxygen functionalities of graphene oxide and TiO_2 nanoparticles [39].

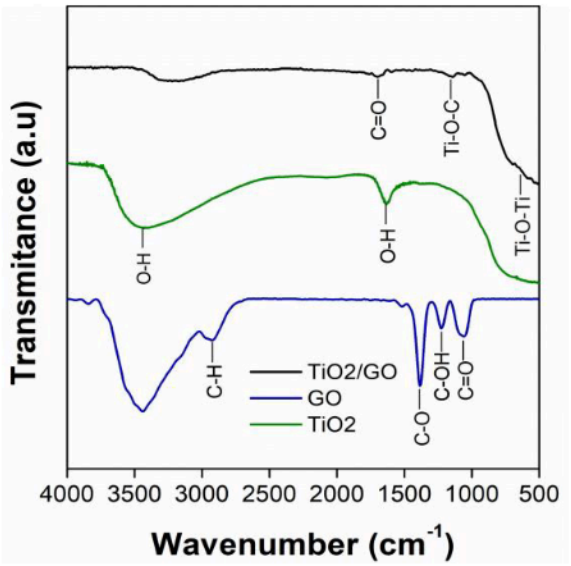

Figure. 2. FTIR of the materials synthesized in this study: TiO_2/GO, GO and TiO_2. Source: Own elaboration.

The thermal stability of the GO and TiO_2/GO was examined by TGA. Figures 3a and 3b show the TGA and DTG results of each type of sample. The weight loss below 100 °C is due to the decomposition of interstitial water [40]. Also, the weight losses between 130 °C and 250 °C correspond to hydroxyl groups (OH) and the initial degradation of carbonyl groups (C=O) [41], [42]. All the samples presented a weight loss in the thermogravimetric curve between 290 °C and 800 °C; however, the change is not significant, and it cannot be observed in the DTG curve. This weight loss is due to the partial elimination of epoxy groups (C-O) [43]. The amount of TiO_2 was determined at 23.2 wt. % by the weight of the inorganic residues at the end of the TGA analysis. The increase in the thermal stability of TiO_2/GO could be due to the presence of Ti-O-C bonds [44].

TGA and FTIR analyses confirmed the presence of oxygen-containing functional groups. These oxygen functionalities can be related to the oxidation of graphite by hydroxyl anions. The OH- anion attacks the sp^2 carbon atoms at the edge of graphite rods, causing the expansion of layers [45]. The presence of oxygenated functional groups favors the stability of GO in an aqueous medium since these groups make GO hydrophilic [46], [47].

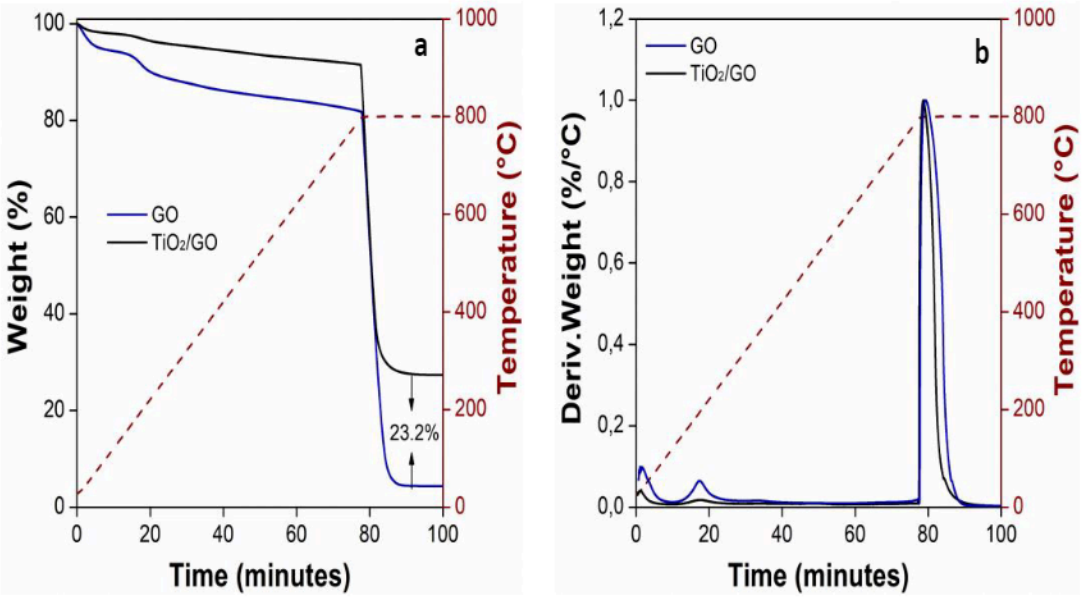

Figure. 3. TGA and DTG spectra of GO and the TiO_2/GO composite. Source: Own elaboration.

The morphology of the materials analyzed in this study was evaluated by SEM and TEM. Figures 4a, 4b, and 4c are SEM micrographs of TiO_2, GO and the TiO_2/GO composite, respectively. Figure 4a reveals that TiO_2 nanoparticles have a spherical morphology. On the other hand, the micrograph of GO (Figure 4b) shows a thin graphene oxide layer; as a result, the background is visible. The micrograph of TiO_2/GO (Figure 4c) presents TiO_2 nanoparticles deposited on a GO layer. In addition, the TEM micrograph of GO (Figure 4f) confirms the exfoliation of graphite rods, which is a that involves the evolution of several gaseous species (SO_2, O_2, CO and CO_2) between layers. These species come from the reduction of the SO_4^{-2} anion, water oxidation and carbon corrosion [48]. In addition, the TEM micrographs and the Raman analysis confirm the presence of few-layer graphene oxide.

The average diameter of the TiO_2 particles in the SEM images was measured by ImageJ software using more than 250 nanoparticles. Figure 4g shows the mean particle size: 24.1 ± 4.6 nm.

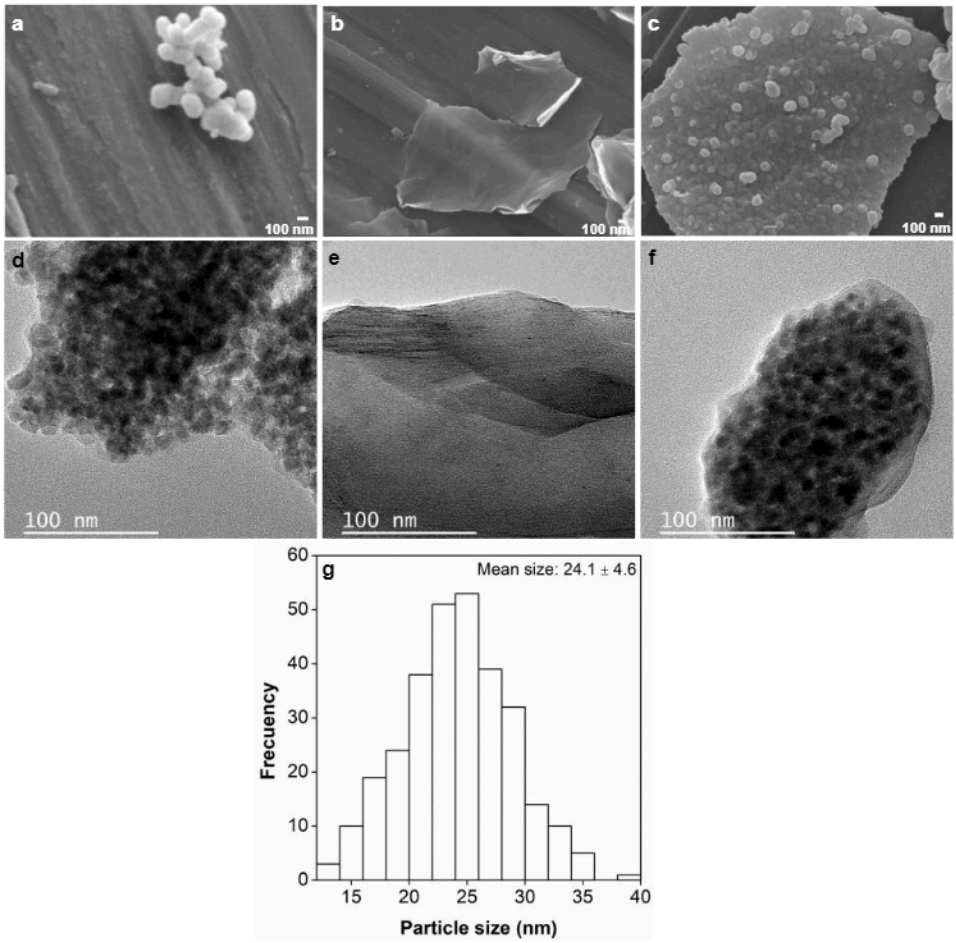

Figure 4. SEM micrographs of (a) TiO_2, (b) GO and (c) the TiO_2/GO composite. TEM micrographs of (d) TiO_2, (e) GO and (f) the TiO_2/GO composite (g) Histogram of TiO_2 particle size distribution.
Source: Own elaboration.

The chemical composition of the TiO_2/GO composite was obtained by Energy Dispersive X-ray Spectroscopy (EDS). Figure 5 shows the EDS spectrum of the hybrid nanomaterial NM and Ti; O and C were found in the sample. Additionally, sodium (Na), which can also be observed in the spectrum, is related to remnants of electrolyte (Na_2SO_4) used during the synthesis of graphene oxide.

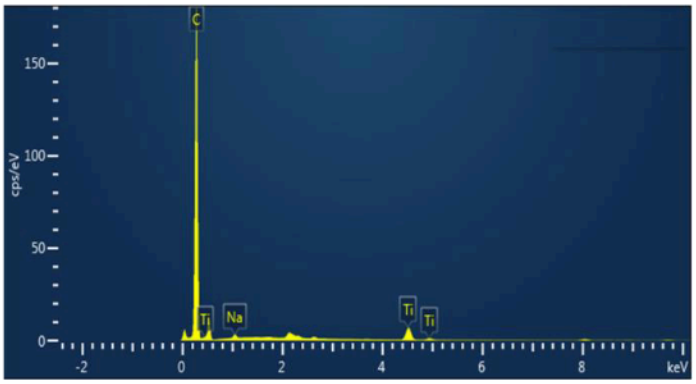

Figure 5. Representative energy dispersive spectrum (EDS) of the TiO_2/GO composite.
Source: Own elaboration.

Figure 6 shows the element distribution map obtained from the TiO_2/GO composite. The map identified the same elements found in the EDS spectrum (C, Ti, O and Na). In addition, the maps clearly show that the nanoparticles of titanium dioxide are located on the surface of the GO layers.

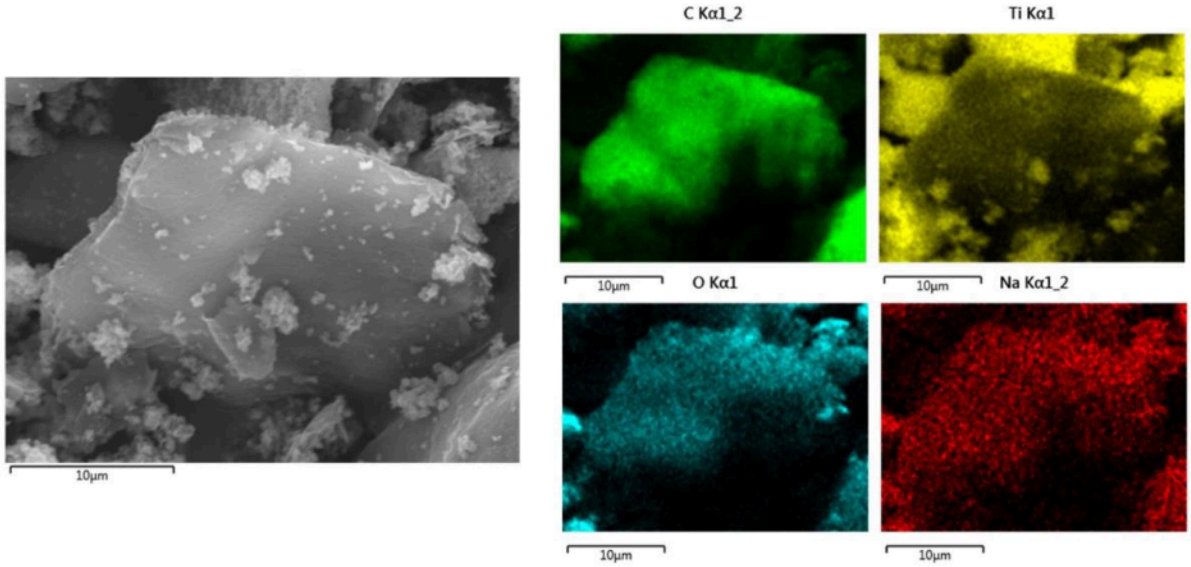

Figure 6. Representative element distribution map of the TiO_2/GO composite. Source: Own elaboration.

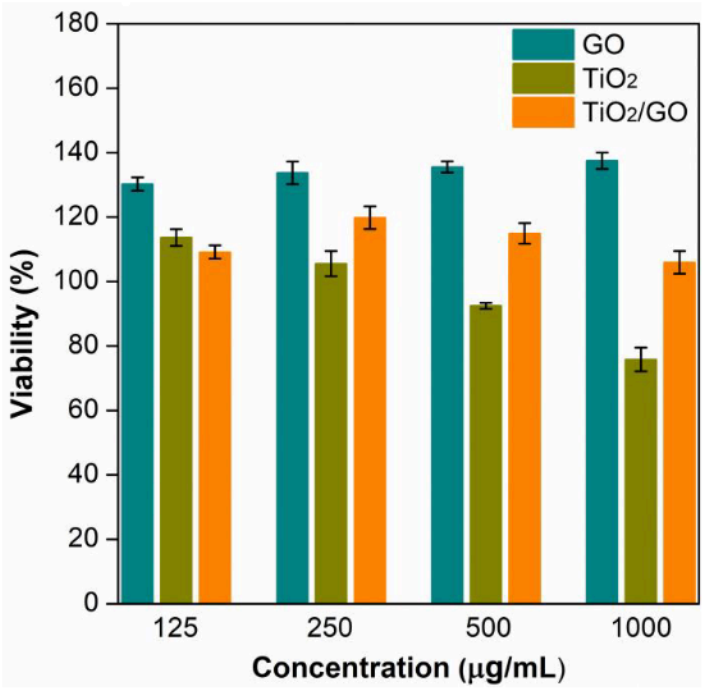

Figure 7. Viability of *E. coli* subjected to GO, TiO_2 and the TiO_2/GO composite. Source: Own elaboration.

The antibacterial activity of the samples prepared here was determined by the macrodilution method. Figure 7 shows the bacterial viability of *E. coli* under different concentrations of GO, TiO_2 and TiO_2/GO. In the results, the graphene oxide sample presents an increase in the viability of *E. Coli* when the concentration of the treatment is higher.

However, the TiO_2 nanoparticles show an inverse trend, i.e., the viability of *E. Coli* decreases as the concentration of nanoparticles increases. At the lowest concentration (i.e., 125 μg/mL), the viability of the bacteria in the TiO_2/GO hybrid material was 23 % and 17 % lower than in the GO and TiO_2 samples, respectively. Nonetheless, at higher concentrations (250, 500 and 1000 μg / mL), the antibacterial activity increased in GO samples but decreased in samples containing TiO_2 nanoparticles. These results indicate that each treatment follows a different trend in terms of bactericidal activity as a function of concentration.

The antibacterial activity of graphene oxide (GO) reported in several papers is controversial. Nevertheless, such activity can be explained by three main mechanisms: membrane rupture, oxidative stress and isolation of bacteria envelope [49]–[51]. The high antibacterial efficacy of graphene oxide is due to the damage it causes to cell membranes through the generation of reactive oxygen species and sharp edges of graphene oxide [49], [52], [53]. In contrast, a large number of studies indicate that this material can promote bacterial growth due to its surface functional groups and because it can act as a scaffold for bacterial attachment, proliferation, and biofilm [49], [54]–[57], which could explain the results reported in this paper.

On the other hand, TiO_2 nanoparticles affect biological systems since their photocatalytic activity generates potential reactive oxygen species (ROS) on their surfaces. ROS cause peroxidation of phospholipids in the cell membrane, inducing its breakdown [58], [59]. The membrane rupture causes the interruption of cellular respiration. For this reason, TiO_2 nanoparticles have a strong antibacterial activity, which is in line with the results reported here, where they achieved the greatest reduction in bacterial viability.

Finally, the behavior of the composite material was similar to that reported by [50] and [60] because carbon blocks the active sites on the surface of TiO_2. Therefore, the contact between the TiO_2 surface and the bacteria can be very limited.

In addition, MIC50 is the minimum amount of drug/compound to inhibit 50 % of microorganism growth and was calculated. GO MIC50 could not be determined because bacterial viability does not decrease with increasing concentration. The MIC50 of TiO_2/GO and TiO_2 was 4575 μg/mL and 1728 μg/ mL, respectively, which confirms that TiO_2 shows a higher bactericidal activity than GO and TiO_2/GO.

4. CONCLUSIONS

This study assessed the effect of TiO_2, GO, and TiO_2/GO nanocompounds on bacterial activity against Escherichia coli. Using the hydrothermal method, TiO_2 nanoparticles were obtained with an anatase phase and an average size of 24.1 ± 4.6 nm. Graphene oxide was obtained through electrochemical exfoliation, a simple and environmentally friendly method that induced a lower amount of oxygen-containing functional groups on the GO surface. A 23.2 % TiO_2 content was evidenced in the developed hybrid nanomaterial. Furthermore, GO promoted bacterial growth due to its surface functional groups. TiO_2 exhibited stronger bactericidal activity than the TiO_2/GO compound. This behavior may be associated with the decreased contact between TiO_2 and bacterial cells due to the blocking of active sites on the TiO_2 surface by graphene sheets.

5. ACKNOWLEDGMENTS

The authors would like to thank the Polymers Laboratory and the Advanced Materials and Energy Research Group (MATyER) at the Instituto Tecnológico Metropolitano (Medellín, Colombia) for providing the chemical reagents and infrastructure used in this research.

CONFLICTS OF INTEREST

None of the authors have any conflict of interests regarding the publication of this work.

AUTHOR CONTRIBUTIONS

G. Durango-Giraldo, C. Zapata-Hernandez, C. Betancur-Henao. Contributed equally to this work. Roles: Investigation, Methodology, Validation, Writing – original draft.

J.F Santa-Marín and R. Buitrago-Sierra. Contributed equally to this work. Roles: Conceptualization, Formal analysis, Investigation, Methodology, Supervision, Validation, Writing – review & editing.

6. REFERENCES

[1] H. A. Khan, A. Ahmad, and R. Mehboob, "Nosocomial infections and their control strategies," *Asian Pac. J. Trop. Biomed.*, vol. 5, no. 7, pp. 509–514, Jul. 2015. https://doi.org/10.1016/j.apjtb.2015.05.001

[2] S. L. Percival, and D. W. Williams, "Escherichia coli," in *Microbiology of Waterborne Diseases,* Elsevier, 2014, pp. 89–117. https://doi.org/10.1016/B978-0-12-415846-7.00006-8

[3] E. P. Dellinger, "Prevention of Hospital-Acquired Infections," *Surg Infect (Larchmt).*, vol. 17, no. 4, pp. 422–426, Jul. 2016. https://doi.org/10.1089/sur.2016.048

[4] Z. Chao, W. Xinru, L. Aihui, C. Pan, H. Ding, and Y. Wei, "Reduced graphene oxide/titanium dioxide hybrid nanofiller-reinforced electrospun silk fibroin scaffolds for tissue engineering - ScienceDirect," *Mater. Lett.*, vol. 291, p. 129563, May. 2021. https://doi.org/10.1016/j.matlet.2021.129563

[5] C. Ying-Na *et al.*, "Synthesis of magnetic graphene oxide-TiO 2 and their antibacterial properties under solar irradiation," *Appl. Surf. Sci.*, vol. 343, pp. 1–10, Jul. 2015. https://doi.org/10.1016/j.apsusc.2015.03.082

[6] H. Mohammed *et al.*, "Antimicrobial Mechanisms and Effectiveness of Graphene and Graphene-Functionalized Biomaterials. A Scope Review," *Front. Bioeng. Biotechnol.*, vol. 8, May. 2020. https://doi.org/10.3389/fbioe.2020.00465

[7] H. M. Hegab, A. Elmekawy, L. Zou, D. Mulcahy, C. P. Saint, and M. Ginic-Markovic, "The controversial antibacterial activity of graphene-based materials," *Carbon N. Y.*, vol. 105, pp. 362–376, Aug. 2016. https://doi.org/10.1016/j.carbon.2016.04.046

[8] J. Qiu, L. Liu, H. Zhu, and X. Liu, "Combination types between graphene oxide and substrate affect the antibacterial activity," *Bioactive Materials*, vol. 3, no. 3, pp. 341–346, Sep. 2018. https://doi.org/10.1016/j.bioactmat.2018.05.001

[9] A. A. Menazea, and M. K. Ahmed, "Synthesis and antibacterial activity of graphene oxide decorated by silver and copper oxide nanoparticles," *J. Mol. Struct.*, vol. 1218, p. 128536, Oct. 2020. https://doi.org/10.1016/j.molstruc.2020.128536

[10] K. Zhu, H. Tian, X. Zheng, L. Wang, and X. Wang, "Triangular silver nanoparticles loaded on graphene oxide sheets as an antibacterial film," *Materials Letters,* vol. 275, p. 128162, Sep. 2020. https://doi.org/10.1016/j.matlet.2020.128162

[11] H. Feng, R. Cheng, X. Zhao, X. Duan, and J. Li, "A low-temperature method to produce highly reduced graphene oxide," *Nat. Commun.*, vol. 4, p.1539, Feb. 2013. https://doi.org/10.1038/ncomms2555

[12] M. J. Fernández-Merino *et al.*, "Vitamin C is an ideal substitute for hydrazine in the reduction of graphene oxide suspensions," *Journal of Physical Chemistry C.*, vol. 114, no. 14, pp. 6426–6432, Mar. 2010. https://doi.org/10.1021/jp100603h

[13] C. Xu, X. Shi, A. Ji, L. Shi, C. Zhou, and Y. Cui, "Fabrication and characteristics of reduced graphene oxide produced with different green reductants," *PLoS One*, vol. 10, no. 12, p. e0144842, Dec. 2015. https://doi.org/10.1371/journal.pone.0144842

[14] V. Likodimos, "Photonic crystal-assisted visible light activated TiO2photocatalysis," *Appl. Catal. B: Environmental.*, vol. 230, pp. 269–303, Aug. 2018. https://doi.org/10.1016/j.apcatb.2018.02.039

[15] C. Dette *et al.*, "TiO2 Anatase with a Bandgap in the Visible Region," *Nano. Lett.*, vol. 14, no. 11, pp. 6533–6538, Sep. 2014. https://doi.org/10.1021/nl503131s

[16] U. Diebold, "The surface science of titanium dioxide," *Surf. Sci. Rep.*, vol. 48, no. 5–8, pp. 53–229, Jan. 2003. https://doi.org/10.1016/S0167-5729(02)00100-0

[17] A. J. Haider, Z. N. Jameel, and I. H. M. Al-Hussaini, "Review on: Titanium dioxide applications," *Energy Procedia*, vol. 157, pp. 17–29, Jan. 2019. https://doi.org/10.1016/j.egypro.2018.11.159

[18] T. Gakhar, and A. Hazra, "p-TiO2/GO heterojunction based VOC sensors: A new approach to amplify sensitivity in FET structure at optimized gate voltage," *Measurement*, vol. 182, p. 109721, Sep. 2021. https://doi.org/10.1016/J.MEASUREMENT.2021.109721

[19] Y. Sang *et al.*, "Enhanced photocatalytic property of reduced graphene oxide/TiO2 nanobelt surface heterostructures constructed by an in situ photochemical reduction method," *Small*, vol. 10, no. 18, pp. 3775–3782, Sep. 2014. https://doi.org/10.1002/SMLL.201303489

[20] W. Fan, Q. Lai, Q. Zhang, and Y. Wang, "Nanocomposites of TiO2 and Reduced Graphene Oxide as Efficient Photocatalysts for Hydrogen Evolution," *Journal of Physical Chemistry C*, vol. 115, no. 21, pp. 10694–10701, May. 2011. https://doi.org/10.1021/JP2008804

[21] M. Karimi-Nazarabad, E. K. Goharshadi, and M. Aziznezhad, "Solar Mineralization of Hard-Degradable Amphetamine Using TiO2/RGO Nanocomposite," *ChemistrySelect*, vol. 4, no. 48, pp. 14175–14183, Dec. 2019. https://doi.org/10.1002/SLCT.201903943

[22] Y. Jia, C. Hu, P. Shi, Q. Xu, W. Zhu, and R. Liu, "Effects of cellulose nanofibrils/graphene oxide hybrid nanofiller in PVA nanocomposites," *Int. J. Biol. Macromol.*, vol. 161, pp. 223–230, Oct. 2020. https://doi.org/10.1016/J.IJBIOMAC.2020.06.013

[23] I. Kartini, P. Meredith, J. C. D. Da Costa, and G. Q. Lu, "A novel route to the synthesis of mesoporous titania with full anatase nanocrystalline domains," *J. Solgel. Sci. Technol.*, vol. 31, no. 1-3, pp. 185–189, Aug. 2004. https://doi.org/10.1023/B:JSST.0000047984.60654.a1

[24] G. Durango-Giraldo, A. Cardona, J. F. Zapata, J. F. Santa, and R. Buitrago-Sierra, "Titanium dioxide modified with silver by two methods for bactericidal applications," *Heliyon*, vol. 5, no. 5, p. e01608, May. 2019. https://doi.org/10.1016/j.heliyon.2019.e01608

[25] R. Boardman, and R. A. Smith, "Evaluating the efficacy of an essential oil extract of thyme (Thymus vulgaris) against methicillin-sensitive and methicillin-resistant strains of Staphylococci," *American Journal of Essential Oils and Natural Products*, vol. 4, no. 2, pp. 17–22, Apr. 2016. https://www.essencejournal.com/pdf/2016/vol4issue2/PartA/4-2-3-902.pdf

[26] C. Zapata-Hernandez, G. Durango-Giraldo, K. Cauca, and R. Buitrago-Sierra, "Influence of graphene oxide synthesis methods on the electrical conductivity of cotton/graphene oxide composites," *The Journal of The Textile Institute*, vol. 113, no. 1, pp. 131-140, Dec. 2020. https://doi.org/10.1080/00405000.2020.1865507

[27] X. Wei, G. Zhu, J. Fang, and J. Chen, "Synthesis, characterization, and photocatalysis of well-dispersible phase-pure anatase TiO2 nanoparticles," *International Journal of Photoenergy*, vol. 2013, Apr. 2013. https://doi.org/10.1155/2013/726872

[28] S. E. Bourdo *et al.*, "Physicochemical characteristics of pristine and functionalized graphene," *Journal of Applied Toxicology*, vol. 37, no. 11, pp. 1288–1296, Nov. 2017. https://doi.org/10.1002/jat.3493

[29] Y. Z. N. Htwe, W. S. Chow, Y. Suda, A. A. Thant, and M. Mariatti, "Effect of electrolytes and sonication times on the formation of graphene using an electrochemical exfoliation process," *Applied Surface Science*, vol. 469. pp. 951–961, Mar. 2019. https://doi.org/10.1016/j.apsusc.2018.11.029

[30] K. K. De Silva, H. Hsin-Hui, S. Suzuki, and M. Yoshimura, "Ethanol-assisted restoration of graphitic structure with simultaneous thermal reduction of graphene oxide," *Jpn. J. Appl. Phys.*, vol. 57, no. 8S1, p. 08NB03, Jun. 2018. https://doi.org/10.7567/JJAP.57.08NB03

[31] A. Ilnicka, M. Skorupska, P. Kamedulski, and J. P. Lukaszewicz, "Electro-exfoliation of graphite to graphene in an aqueous solution of inorganic salt and the stabilization of its sponge structure with poly(Furfuryl alcohol)," *Nanomaterials*, vol. 9, no. 7, p. 971, Jul. 2019. https://doi.org/10.3390/nano9070971

[32] X. Mei, X. Meng, and F. Wu, "Hydrothermal method for the production of reduced graphene oxide," *Physica E: Low-Dimens Syst Nanostruct.*, vol. 68, pp. 81–86, Apr. 2015. https://doi.org/10.1016/j.physe.2014.12.011

[33] R. Kumar *et al.*, "Bulk synthesis of highly conducting graphene oxide with long range ordering," *RSC Adv.*, vol. 5, no. 45, pp. 35893–35898, Apr. 2015. https://doi.org/10.1039/c5ra01943e

[34] K. Min-Sik, W. Jeong-Min, G. Dae-Myeong, J. R. Rani, and J. Jae-Hyung, "Effect of copper surface pre-treatment on the properties of CVD grown graphene," *AIP Adv.*, vol. 4, no. 12, Dec. 2014. https://doi.org/10.1063/1.4903369

[35] J. R. Anasdass, P. Kannaiyan, R. Raghavachary, S. C. B. Gopinath, and Y. Chen, "Palladium nanoparticle-decorated reduced graphene oxide sheets synthesized using Ficus carica fruit extract: A catalyst for Suzuki cross-coupling reactions," *PLoS One*, vol. 13, no. 2, p. e0193281, Feb. 2018. https://doi.org/10.1371/journal.pone.0193281

[36] S. A. Khan *et al.*, "Synthesis of TiO2/Graphene oxide nanocomposites for their enhanced photocatalytic activity against methylene blue dye and ciprofloxacin," *Compos. B. Eng.*, vol. 175, p. 107120, Oct. 2019. https://doi.org/10.1016/j.compositesb.2019.107120

[37] T. Lling-Lling, O. Wee-Jun, C. Siang-Piao, and A. R. Mohamed, "Reduced graphene oxide-TiO2 nanocomposite as a promising visible-light-active photocatalyst for the conversion of carbon dioxide," *Nanoscale Res. Lett.*, vol. 8, no. 1, p. 465, Nov. 2013. https://doi.org/10.1186/1556-276X-8-465

[38] K. K. Abbas, and A. M. H. A. Al-Ghaban, "Enhanced solar light photoreduction of innovative TiO2 nanospherical shell by reduced graphene oxide for removal silver ions from aqueous media," *Journal of Environmental Chemical Engineering*, vol. 7, no. 3, p. 103168, Jun. 2019. https://doi.org/10.1016/j.jece.2019.103168

[39] Y. Ren, L. Zhao, Y. Zou, L. Song, N. Dong, and J. Wang, "Effects of different TiO2 particle sizes on the microstructure and optical limiting properties of TiO2/reduced graphene oxide nanocomposites," *Nanomaterials*, vol. 9, no. 5, p.730, May. 2019. https://doi.org/10.3390/nano9050730

[40] M. P. Lavin-Lopez, A. Paton-Carrero, L. Sanchez-Silva, J. L. Valverde, and A. Romero, "Influence of the reduction strategy in the synthesis of reduced graphene oxide," *Advanced Powder Technology*, vol. 28, no. 12, pp. 3195–3203, Dec. 2017. https://doi.org/10.1016/j.apt.2017.09.032

[41] R. Larciprete, P. Lacovig, S. Gardonio, A. Baraldi, and S. Lizzit, "Atomic oxygen on graphite: Chemical characterization and thermal reduction," *Journal of Physical Chemistry C*, vol. 116, no. 18, pp. 9900–9908, Apr. 2012. https://doi.org/10.1021/jp2098153

[42] C. Botas *et al.*, "Critical temperatures in the synthesis of graphene-like materials by thermal exfoliation-reduction of graphite oxide," *Carbon N. Y.*, vol. 52, p. 476-485, Feb. 2013. https://doi.org/10.1016/j.carbon.2012.09.059

[43] G. Zhang, M. Wen, S. Wang, J. Chen, and J. Wang, "Insights into thermal reduction of the oxidized graphite from the electro-oxidation processing of nuclear graphite matrix," *RSC Adv.*, vol. 8, no. 1, pp. 567–579, Jan. 2018. https://doi.org/10.1039/c7ra11578d

[44] V. Z. Baldissarelli, T. De Souza, L. Andrade, L. F. C. De Oliveira, H. J. José, and R. D. F. P. Muniz Moreira, "Preparation and photocatalytic activity of TiO 2 -exfoliated graphite oxide composite using an ecofriendly graphite oxidation method," *Applied Surface Science,* vol. 359, pp. 868–874, Dec. 2015. https://doi.org/10.1016/j.apsusc.2015.10.199

[45] P. Yu, S. E. Lowe, G. P. Simon, and Y. L. Zhong, "Electrochemical exfoliation of graphite and production of functional graphene," *Curr. Opin. Colloid Interface Sci.*, vol. 20, no. 5–6, pp. 329–338, Oct-Dec. 2015. https://doi.org/10.1016/j.cocis.2015.10.007

[46] L. Qiu *et al.*, "Dispersing carbon nanotubes with graphene oxide in water and synergistic effects between graphene derivatives," *Chemistry - A European Journal*, vol. 16, no. 35, pp. 10653–10658, Sep. 2010. https://doi.org/10.1002/chem.201001771

[47] N. Keklikcioglu Cakmak, "The impact of surfactants on the stability and thermal conductivity of graphene oxide de-ionized water nanofluids," *J. Therm. Anal. Calorim.*, vol. 139, no. 3, pp. 1895–1902, Dec. 2020. https://doi.org/10.1007/s10973-019-09096-6

[48] H. Lee, J. I. Choi, J. Park, S. S. Jang, and S. W. Lee, "Role of anions on electrochemical exfoliation of graphite into graphene in aqueous acids," *Carbon N. Y.*, vol. 167, pp. 816–825, Oct. 2020. https://doi.org/10.1016/j.carbon.2020.06.044

[49] M. Yousefi *et al.*, "Anti-bacterial activity of graphene oxide as a new weapon nanomaterial to combat multidrug-resistance bacteria," *Materials Science and Engineering C Mater. Biol. Appl.*, vol. 74. pp. 568–581, May. 2017. https://doi.org/10.1016/j.msec.2016.12.125

[50] N. S. Ahmad, N. Abdullah, and F. M. Yasin, "Toxicity assessment of reduced graphene oxide and titanium dioxide nanomaterials on gram-positive and gram-negative bacteria under normal laboratory lighting condition," *Toxicology Reports,* vol. 7, pp. 693–699, 2020. https://doi.org/10.1016/j.toxrep.2020.04.015

[51] A. Khan, F. Ameen, F. Khan, A. Al-Arfaj, and B. Ahmed, "Fabrication and antibacterial activity of nanoenhanced conjugate of silver (I) oxide with graphene oxide," *Mater. Today Commun.*, vol. 25, p. 101667, Dec. 2020. https://doi.org/10.1016/j.mtcomm.2020.101667

[52] H. Zheng *et al.*, "Antibacterial applications of graphene oxides: structure-activity relationships, molecular initiating events and biosafety," *Science Bulletin*, vol. 63, no. 2. pp. 133–142, Jan. 2018. https://doi.org/10.1016/j.scib.2017.12.012

[53] C. Xie *et al.*, "Elucidating the origin of the surface functionalization - dependent bacterial toxicity of graphene nanomaterials: Oxidative damage, physical disruption, and cell autolysis," *Science of the Total Environment*, vol. 747, p. 141546, Dec. 2020. https://doi.org/10.1016/j.scitotenv.2020.141546

[54] T. Zhang, and T. Pier-Luc, "Graphene: An Antibacterial Agent or a Promoter of Bacterial Proliferation?," *iScience*, vol. 23, no. 12, p. 101787, Dec. 2020. https://doi.org/10.1016/j.isci.2020.101787

[55] H. Luo, H. Ao, M. Peng, F. Yao, Z. Yang, and Y. Wan, "Effect of highly dispersed graphene and graphene oxide in 3D nanofibrous bacterial cellulose scaffold on cell responses: A comparative study," *Mater. Chem. Phys.*, vol. 235, p. 121774, Sep. 2019. https://doi.org/10.1016/j.matchemphys.2019.121774

[56] A. Raja C. *et al.*, "Decoration of 1-D nano bioactive glass on reduced graphene oxide sheets: Strategies and in vitro bioactivity studies," *Materials Science and Engineering C Mater. Biol. Appl.*, vol. 90, pp. 85–94, Sep. 2018. https://doi.org/10.1016/j.msec.2018.04.040

[57] O. N. Ruiz *et al.*, "Graphene oxide: a nonspecific enhancer of cellular growth," *ACS Nano*, vol. 5, no. 10, pp. 8100–8107, Sep. 2011. https://doi.org/10.1021/nn202699t

[58] V. Scuderi *et al.*, "Photocatalytic and antibacterial properties of titanium dioxide flat film," *Mater. Sci. Semicond. Process.*, vol. 42, pp. 32–35, Feb. 2016. https://doi.org/10.1016/j.mssp.2015.09.005

[59] Y. H. Leung *et al.*, "Toxicity of ZnO and TiO2 to Escherichia coli cells.," *Sci. Rep.*, vol. 6, p. 35243, Oct. 2016. https://doi.org/10.1038/srep35243

[60] A. Wanag *et al.*, "Antibacterial properties of TiO2 modified with reduced graphene oxide," *Ecotoxicology and Environmental Safety*, vol. 147, pp. 788–793, Jan. 2018. https://doi.org/10.1016/j.ecoenv.2017.09.039